



HAL
open science

Temporal changes in zooplankton indicators highlight a bottom-up process in the Bay of Marseille (NW

Théo Garcia, Daniela Banaru, Loïc Guilloux, Véronique Cornet, Gérald Gregori, François Carlotti

► To cite this version:

Théo Garcia, Daniela Banaru, Loïc Guilloux, Véronique Cornet, Gérald Gregori, et al.. Temporal changes in zooplankton indicators highlight a bottom-up process in the Bay of Marseille (NW. PLoS ONE, 2023, 18 (10), pp.e0292536. 10.1371/journal.pone.0292536 . hal-04255762

HAL Id: hal-04255762

<https://hal.science/hal-04255762>

Submitted on 24 Oct 2023

HAL is a multi-disciplinary open access archive for the deposit and dissemination of scientific research documents, whether they are published or not. The documents may come from teaching and research institutions in France or abroad, or from public or private research centers.

L'archive ouverte pluridisciplinaire **HAL**, est destinée au dépôt et à la diffusion de documents scientifiques de niveau recherche, publiés ou non, émanant des établissements d'enseignement et de recherche français ou étrangers, des laboratoires publics ou privés.

1 Temporal changes in zooplankton indicators highlight a
2 bottom-up process in the Bay of Marseille (NW
3 Mediterranean Sea).

4 Théo GARCIA^{1*¶}, Daniela BĂNARU^{1¶}, Loïc GUILLOUX^{1&},
5 Véronique CORNET^{1&}, Gérald GREGORI^{1&}, François CARLOTTI^{1¶}

6 *(1) Aix-Marseille Université, Université de Toulon, CNRS/INSU,*
7 *IRD, Mediterranean Institute of Oceanography (MIO), UM 110,*
8 *Campus universitaire de Luminy, Marseille, France*

9 *Corresponding author: theo.garcia@mio.osupytheas.fr (TG)

10

11 **Abstract**

12 Sixteen years (2005-2020) of zooplankton monitoring in the Bay of Marseille (N-W
13 Mediterranean Sea) are analyzed in relation to physical, meteorological, climatic and biotic
14 data. Samples were collected every two weeks by a vertical haul (0-55 m) of a 200 μm plankton
15 net. Different indices characterizing the mesozooplankton are compared: biomass dry weight
16 of four size fractions between 200 and 2000 μm ; abundances of the whole of the
17 mesozooplankton and of 13 main taxonomic groups defined from plankton imagery; seasonal
18 onset timing of each zooplankton group; and two other types of indices, the first characterized
19 diversity based on abundance data; and the second derived from zooplankton size spectra shape.
20 The multi-indices approach showed different dynamics and the indices were complementary to
21 disentangle changes in zooplankton. While the biomass of the four mesozooplankton size
22 fractions decreased over the whole period of study, total abundance first decreased slightly but
23 then increased at the end of the period. The reduced dominance of copepods (calanoids and
24 oithonoids) and the increase in abundance of other taxonomic groups (particle feeders,
25 omnivores and carnivores) induced a higher diversity over time. The mesozooplankton size
26 spectra shifted towards smaller sizes in 2009, when the 1000-2000 μm size fraction biomass
27 decreased, and moved again towards larger sizes in 2012 along with increased diversity. Joint
28 analysis with environmental indices over the period of study showed a decrease of particulate
29 organic matter, and changes in phytoplankton size structure towards smaller sizes, coinciding
30 with changes in nutrient stoichiometry and decreasing concentrations. In addition, from 2013
31 the seasonal onset of several zooplankton groups occurred later. The delayed zooplankton
32 seasonal cycles were shown as concomitant with increasing winter temperatures, precipitation
33 and NAO. Our results supported the hypothesis of bottom-up control in the pelagic ecosystem
34 in the NW-Mediterranean Sea.

35 **1-Introduction**

36 Zooplankton are short-lived organisms, highly sensitive to environmental changes, which
37 makes their long-term monitoring an excellent approach to provide responses to management
38 issues [1,2]. Previous time series analyses have shown that zooplankton shifts can be observed
39 at various scales: at large scale through climate-related processes [3,4], at regional scale in
40 relation with regional meteorological phenomena, and at local scale (e.g. bays) most often in
41 response to human pressure [5,6]. These multiple stressors alter the physiology, behavior and
42 phenology of organisms, and consequently population distributions [7,8]. Nonetheless the
43 multiple scales of forcing make it difficult to disentangle causation.

44 The increase in zooplankton observations has made it possible to validate several indicators
45 such as those based on individual taxa, species assemblages, diversity indices or size spectra,
46 which are useful for characterizing the state of pelagic ecosystems [1]. The development of
47 multi-indicator approaches has made it possible to better compare them, and thus to identify
48 their complementary contributions. Therefore nowadays quantification of the roles of
49 zooplankton in biogeochemical fluxes and trophic fluxes towards higher levels requires, in
50 addition to information on biomass and size spectra, knowledge of taxonomic distributions and
51 associated ecological traits.

52 In the Gulf of Lion (NW Mediterranean), earlier studies dedicated to zooplankton were focused
53 on quantification of either biogeochemical flux or pelagic trophic flows, and were all carried
54 out during oceanographic cruises over short periods (less than a month)[9–19]. Recent
55 increased interest in the role of zooplankton as trophic resources for planktivorous fish has been
56 prompted by the reduction in size of two planktivorous fishes (European pilchard, *Sardina*
57 *pilchardus*, and European anchovy, *Engraulis encrasicolus*) in the Gulf of Lion in 2008 (NW
58 Mediterranean) [20–23]. Various studies have led to rejection of the hypotheses of the impact
59 of overfishing, increased predation, disease and a decline in recruitment [24]. The observation

60 of a drastic reduction in the size of individuals [20,24,25] has been linked to a deficit in
61 individual growth attributed to potential changes in plankton resources, although this has not
62 yet been proven. To shed light on this potential planktonic change, the data from oceanographic
63 cruises over the last few decades in the Gulf of Lion are too few and limited in time, and the
64 closest locations of zooplankton monitoring time series in the Ligurian Sea [4,26,27] or the
65 Balearic Sea [28] are far apart.

66 A mesozooplankton monitoring survey that has been carried out since 2005 in the Bay of
67 Marseille (BoM) provides a zooplankton time series in the Gulf of Lion which encompasses
68 the critical shift period. Zooplankton sampling was added to an existing monitoring programme
69 started in 1994 including hydrological and nutrient measurements, as well as sampling for a
70 few biotic variables (pigment, bacteria and phytoplankton). The sampling station at the center
71 of the BoM is subject to multiple regional environmental influences such as winter deep
72 convection phenomena from the Provencal basin off the Gulf of Lion, north-westerly winds
73 (known as Mistral), which induce coastal upwelling events [29], intrusions from the Rhone
74 River under certain wind conditions [30], intrusions from the northerly current from the
75 Ligurian Sea [31], and local anthropogenic influences due to the proximity of the Marseille
76 agglomeration (e.g. sewage plants)[32].

77 In this paper, we aimed to test the hypothesis of a bottom-up relationship between
78 environmental conditions, phytoplankton, and zooplankton in the BoM. To achieve this goal
79 we will first describe a number of zooplankton indices and examine their interannual and
80 seasonal variations in order to identify major changes over the last two decades. We will then
81 relate zooplankton changes to variations in other monitored abiotic and biotic parameters, and
82 discuss how the observed changes might be the result of bottom-up forcing. Finally, we will
83 discuss how this could affect planktivorous fish.

84 2-Material and methods

85 2.1- Environmental data

86 Sampling was carried out in the Bay of Marseille (N-W Mediterranean Sea) at the Frioul
87 monitoring station (60m depth, 43.24°N; 5.29°E) of the long-term national littoral observation
88 program SOMLIT (www.somlit.fr), in the eastern part of the Gulf of Lion (Fig 1). This
89 monitoring survey has generated an extensive collection of physical, chemical, and biological
90 data (see summary of the variables in Table 1). Twice a month since 1994, a vertical CTD-
91 oxygen-fluorometer cast of the whole water column (0-55m) and Niskin bottle sampling were
92 performed at three depths (subsurface -1 m-, bottom -55 m- and fluorescence maximum -
93 variable). The values of each measurement obtained at the three depths were averaged. Climatic
94 and meteorological indices completed the environmental database (Table 1).

95 **Fig 1. Map of the study site.** In the left panel, localization of the Bay of Marseille (red) at
96 Basin (NW Mediterranean) and Gulf of Lion scale. In the right panel, localization of the Frioul
97 sampling station in the Bay of Marseille. Color gradient refers to the bathymetry on the left
98 panel. Maps were produced using Natural Earth and France-GeoJSON [33] open access data.

99 **Table 1: Summary of the variables used in this study.**

Variable	Abbreviation	Unit	Category	Time	Source
Wind stress (according to NW-SE axis)	Wind stress	-	Environmental	2005-2020	Calculation from Météo France
Precipitation	Prec	mm	Environmental	2005-2020	Météo France
Mixed Layer Depth	MLD	m	Environmental	2005-2020	Calculation from SOMLIT data
Western Mediterranean Oscillation	WeMO	-	Environmental	2005-2020	[34]
Northern Atlantic Oscillation	NAO	-	Environmental	2005-2020	NOAA
Temperature	T	°C	Environmental	2005-2020	SOMLIT
Salinity	S	-	Environmental	2005-2020	SOMLIT

Oxygen	O	mL.L ⁻¹	Environmental	2005-2020	SOMLIT
Ammonium concentration	NH4	μmol.L ⁻¹	Environmental	2005-2020	SOMLIT
Nitrate concentration	NO3	μmol.L ⁻¹	Environmental	2005-2020	SOMLIT
Nitrite concentration	NO2	μmol.L ⁻¹	Environmental	2005-2020	SOMLIT
Phosphate concentration	PO4	μmol.L ⁻¹	Environmental	2005-2020	SOMLIT
Particulate Organic Carbon	POC	μg.L ⁻¹	Environmental	2005-2020	SOMLIT
Particulate Organic Nitrogen	PON	μg.L ⁻¹	Environmental	2005-2020	SOMLIT
Suspended particulate matter	SPM	μg.L ⁻¹	Environmental	2005-2020	SOMLIT
Chlorophyll a	CHLA	μg.L ⁻¹	Environmental	2005-2020	SOMLIT
Diatoms and diatoms counts (subsurface)	Micro	cells.L ⁻¹	Environmental	2010-2020	SPECIMED [35] and PHYTOBS [36]
Ratio diatoms counts : dinoflagellates counts (subsurface)	Ratio Diat:Dino	-	Environmental	2010-2020	SPECIMED [35] and PHYTOBS [36]
High Nucleic Acid Bacteria counts (subsurface)	HNA bacteria	cells.mL ⁻¹	Environmental	2009-2020	SOMLIT
High Nucleic Acid Bacteria size index (subsurface)	HNA bacteria size	-	Environmental	2009-2020	SOMLIT
Low Nucleic Acid Bacteria counts (subsurface)	LNA bacteria	cells.mL ⁻¹	Environmental	2009-2020	SOMLIT
Low Nucleic Acid Bacteria size index (subsurface)	LNA bacteria size	-	Environmental	2009-2020	SOMLIT
Total Bacteria counts (subsurface)	Tot bacteria	cells.mL ⁻¹	Environmental	2009-2020	SOMLIT
Total Bacteria size index (subsurface)	Tot bacteria size	-	Environmental	2009-2020	SOMLIT
<i>Cryptophyceae</i> counts (subsurface)	Crypto	cells.mL ⁻¹	Environmental	2009-2020	SOMLIT
<i>Cryptophyceae</i> size index (subsurface)	Crypto size	-	Environmental	2009-2020	SOMLIT
<i>Synechococcus</i> counts (subsurface)	Syne	cells.mL ⁻¹	Environmental	2009-2020	SOMLIT
<i>Synechococcus</i> size index (subsurface)	Syne size	-	Environmental	2009-2020	SOMLIT
<i>Prochlorococcus</i> counts (subsurface)	Pro	cells.mL ⁻¹	Environmental	2009-2020	SOMLIT
<i>Prochlorococcus</i> size index (subsurface)	Pro size	-	Environmental	2009-2020	SOMLIT

Picophytoplankton counts (subsurface)	Pico	cells.mL ⁻¹	Environmental	2009-2020	SOMLIT
Picophytoplankton size index (subsurface)	Pico size	-	Environmental	2009-2020	SOMLIT
Nanoplankton counts (subsurface)	Nano	cells.mL ⁻¹	Environmental	2009-2020	SOMLIT
Nanoplankton size index (subsurface)	Nano size	-	Environmental	2009-2020	SOMLIT
Biomass for size fraction 1000-2000µm	Biom 1000-2000	mg of dry weight.m ⁻³	Zooplankton	2005-2020	This study
Biomass for size fraction 500-1000µm	Biom 500-1000	mg of dry weight.m ⁻³	Zooplankton	2005-2020	This study
Biomass for size fraction 300-500µm	Biom 300-500	mg of dry weight.m ⁻³	Zooplankton	2005-2020	This study
Biomass for size fraction 200-300µm	Biom 200-300	mg of dry weight.m ⁻³	Zooplankton	2005-2020	This study
Total Biomass 200-2000 µm	Total Biomass	mg of dry weight.m ⁻³	Zooplankton	2005-2020	This study
Zooplankton size structure (1st PC)	Zoopk PC1	-	Zooplankton	2005-2020	This study
Zooplankton size structure (2nd PC)	Zoopk PC2	-	Zooplankton	2005-2020	This study
Community structure index MDS 1	MDS1	-	Zooplankton	2005-2020	This study
Community structure index MDS 2	MDS2	-	Zooplankton	2005-2020	This study
Community structure index MDS 3	MDS3	-	Zooplankton	2005-2020	This study
Zooplankton abundances	Abundance	individuals.m ⁻³	Zooplankton	2005-2020	This study

100

101 **2.2- Zooplankton data.**

102 In parallel with the SOMLIT monitoring survey, mesozooplankton samples have been collected
103 since 2005 through vertical hauls using a WP2 200 µm mesh size plankton net (water column
104 sampled: 0-55 m). The samples were fractioned in two. The first half of the cod-end content
105 was preserved in a 4% buffered formaldehyde solution for digitalizing; the other half was
106 maintained in cold condition for zooplankton size-fractioned dry weight (biomass)
107 measurements. Complementary information concerning the environmental and zooplankton
108 monitoring is given in the S1 file.

109 **2.2.1-Zooplankton size-fractioned dry weights**

110 The aliquot of cod-end content maintained in marine water was fractioned on a sieve column
111 in 6 size fractions: 80-200 μm , 200-300 μm , 300-500 μm , 500-1000 μm , 1000-2000 μm and
112 $>2000 \mu\text{m}$. The material from each sieve was recovered on pre-combusted and pre-weighed
113 Whatman GF/F filters and dried for 48h at 60°C for biomass measurement. Because the
114 WP2 200 μm mesh size plankton net does not efficiently sample the smallest and largest size
115 fractions, the 80-200 μm and $>2000 \mu\text{m}$ fractions were not considered in our study.

116 **2.2.2-Zooplankton digitalization**

117 The other aliquot conserved in the formaldehyde solution was used for plankton digitalization
118 following the procedure in [37] with a Zooscan. During the image processing, a proxy of
119 individual size has been obtained by means of Equivalent Spherical Diameter (ESD, see [38]).
120 A Convolutional Neural Network (CNN) has been trained for vignette classification [39]. The
121 CNN predicted zooplankton vignettes in the following 13 classes: appendicularians, bivalves,
122 calanoid copepods, ergasilida copepods, harpacticoid copepods, oithonoid copepods, nauplii
123 copepods, crustaceans (which includes holoplankton, e.g. amphipod, cladocera, and
124 meroplankton, e.g. decapod), chaetognaths, cnidarians, fish eggs, pteropods and salps. See the
125 S2 file for more details concerning CNN classification, training, and performance.

126 **2.3- Data analysis**

127 Data analyses were conducted on R software version 4.1.2 [40].

128 **2.3.1-Description of zooplankton community structure indices**

129 Size spectra were constructed using images with ESDs between 200 μm (limit of particle
130 detection by Zooscan) and 1660 μm (i.e. outliers were excluded according to the Tukey method
131 [41]). Following the method described by Nerini and Ghattas [42], the shape of the zooplankton
132 size spectra was studied by means of Functional Principal Component Analysis (FPCA). The

133 FPCA is a statistical tool that ordinales sample units according to the characteristics (i.e. the
134 shape) of their functional entity (i.e. here a curve/size spectrum). This methodology was applied
135 as follows: (i) zooplankton size spectrum densities for all samples were estimated using Kernel
136 density estimator; (ii) the density functions were converted into a continuous functional object,
137 a curve, using 250 B-splines functions; (iii) the curves obtained from all samples were ordinated
138 by means of a FPCA [43]. We applied the FPCA on the coefficients of the B-spline expansion
139 model as explained by Pauthenet et al. in [44]. These new variables which concentrate the
140 variance of the system are the principal components (PCs) and represent the most significant
141 modes of the data variation.

142 The sample scores on the first two PCs were used as time series to describe the variations of
143 the size spectrum shapes and by extension the structure of the zooplankton community size.

144 In addition, multidimensional scaling (MDS) was applied on the species abundance table to
145 disentangle the diversity structure with Manhattan distance. The sample scores of the three
146 MDS axes were used as time series to describe the variations of the diversity structure.

147 The R packages 'fda' [43] and 'vegan' [45] were respectively used to perform the FPCA and
148 MDS analysis.

149 **2.3.2-Exploring interannual changes in zooplankton data**

150 Time series data were averaged on a monthly basis and missing values were imputed using the
151 Multiple Imputation with Principal Component Analysis (MIPCA) procedure using the R
152 package 'MissMDA' [46]. Trends in monthly time series were highlighted using Local
153 Polynomial Regressions (LOESS, using 75% of the neighborhood data). Breakpoint detection
154 procedure ('strucchange' package in R [47]) was applied to highlight the structural change on
155 every single time-series. Until three breakpoints were investigated, the optimum number of
156 breakpoints was defined according to the Bayesian Information Criterion (BIC).

157 **2.3.3- Zooplankton seasonality**

158 Level plots were used to describe seasonal patterns in the various zooplankton series: biomass,
159 abundance (see 2.2- Zooplankton data) and structure descriptors (see 3.1- Community structure
160 indices). In order to obtain a smoothed picture of the level plot, LOESS functions were applied
161 over 30 equally spaced points on the year/month grids. Seasonal patterns were assessed by
162 fitting sinusoidal models. The seasonal pattern was considered significant when the sinusoidal
163 effect was significant (p-value<0.05). The seasonal onset timing of each zooplankton group
164 was defined as the date when 20% of the yearly cumulative value was reached [8,48].

165 **2.3.4- Investigating relationships between environmental and zooplankton** 166 **time series**

167 Dynamic Factor Analysis (DFA, [49]) is a statistical method that aims to find common trends
168 among observational data. In our case DFA was applied in order to find common trends between
169 environmental and zooplankton data. DFA belongs to the family of the state-space models and
170 allows determination of M hidden common trend(s) among N standardized (to reduce the
171 impact of the variable scale on the analysis) data time series, when $M \ll N$. DFA models relate
172 observational time series (y) to the sum of the M hidden trends linear combination and noise.
173 This can be represented by the following equation (1):

$$174 \quad y_t = \Gamma \alpha_t + \varepsilon_t ; \text{where } \varepsilon_t \sim N(0, R) \quad (1)$$

175
176 Γ is a matrix of dimensions $N \times M$ and contains the factor loadings of the N factors for M
177 detected hidden trends, α_t is a vector of length M containing the M common trends at time t. ε_t
178 is the noise component which follows a normal distribution of mean 0 and variance-covariance
179 matrix R.

180 DFA models require user specification for certain parameters:

181 - Firstly, different assumptions on the noise, R, variance-covariance matrix among factors can
182 be made:

183 - same variance and no covariance ('diagonal and equal')

184 - different variances and no covariances ('diagonal and unequal')

185 - same variances and same covariances ('equalvarcov')

186 - different variances and covariances ('unconstrained')

187 -Secondly, the number of M hidden trends must be specified as low as possible to facilitate
188 interpretation ($M \ll N$).

189 Correction of Akaike Information Criterion (AICc) was applied to select the most likely data
190 model.

191 Multiple DFA models were computed on:

192 (1) - all environmental data for the 2005-2020 period. From one to three common trends
193 were investigated among the 34 environmental times series with the four different assumptions
194 on the R matrix. A total of 12 models were computed on environmental time series.

195 (2) - zooplankton data for the 2005-2020 period. From one to three common trends were
196 investigated among 11 zooplankton times series with the four different assumptions on the R
197 matrix. A total of 12 models were computed on biological data.

198 (3) - environmental winter conditions (average values between January and March) and
199 dates of zooplankton seasonal onset. From one to three common trends were investigated
200 among the 34 environmental and 19 zooplankton time series with the four different assumptions
201 on the R matrix. A total of 12 models were computed.

202 As DFA aimed at finding common trends among short time series, in (1) and (2), time series
203 were averaged at a biannual time step. This allowed to reduce the computing time for the
204 models. The series were de-seasonalized (i.e. when seasonal patterns were detected, by means
205 of partial autocorrelation functions) to focus on interannual variations. DFA can be performed

206 with missing data. For model 1 and 3 some time series were shorter (i.e. micro-, pico-, nano-
207 plankton data started in 2009), the results of the models fitting computed for those variables
208 were therefore not discussed before 2009.

209 Dynamic factor analysis models were computed with the MARSS package [50].

210 **3-Results**

211 **3.1-Community structure indices**

212 The two first PCs of the FPCA performed on the size spectra curves explained 66.7% of the
213 data variability (Figs 2A and 2B). In each figure, positive and negative influences of the
214 factorial axes on the size spectra shape are displayed. The variation modes of the size spectra
215 shape on the first axis explained 45.9% of the data variability. Positives values on the first
216 factorial axis (Fig 2 A, red curve) the size spectra were associated with a displacement of size
217 spectra mode towards higher ESD. Negatives values on first factorial axis (Fig 2 A, blue curve)
218 was associated with a displacement of size spectra mode toward lower values. The second axis
219 of the FPCA explained 20.8% of the data variability. Positives values on the second PC (Fig
220 2B, red curve) were associated with the displacement of the size spectra peak toward lower
221 ESD and the increase of the proportion of larger zooplankton organisms (>500 μm ESD).
222 Negative values on the second PC (Fig 2B, blue curve) were associated with the displacement
223 of the size spectra peak toward higher ESD and the decrease of the proportion of larger
224 zooplankton organisms (>500 μm ESD). The MDS (Figs 2C and 2D) computed on the
225 abundances of the thirteen taxa best recognized by the CNN model summarized the structure in
226 species of the zooplankton community (stress <0.2). The ordination method separated in the
227 first axis the centroid of two copepod taxa (calanoids and oithonoids, positive values) to
228 chaetognaths and salps (negative values). The second axis (Fig 2C) separated bivalve, pteropods
229 and harpacticoid centroids (positive values) from all other species centroids. The last axis (Fig

230 2D) discriminated crustacean centroid (positive values) from copepods nauplii centroid
231 (negative values).

232 **Fig 2. Results of the FPCA (A & B) and MDS (C & D) analysis to derive community**
233 **structure indices.** Influence of factorial axis (A for first PC and B for second PC) on the shape
234 of the functional object (size spectra curve). Black line is the mean functional curve of the
235 FPCA. Red curve (+ symbol) and blue curve (- symbol) represent respectively the positive and
236 negative influence of the factorial axis on the size spectra shape. Limits of the x-axis of A & B
237 graphs are set to 200 to 1000 μm , as the main variations of the influence of the factorial axis on
238 the functional object are observable before 1000 μm ESD. Representation of the ordination of
239 the MDS (C: first vs second axis, D: first vs third axis). The black dots correspond to the
240 projections on the 2D space of the samples. The red labels correspond to the centroids position
241 of the *taxa*. *Taxa* abbreviations correspond to the following groups: app: appendicularians; biva:
242 bivalves; cala: calanoids copepods; chae: chaetognaths; cnid: cnidarians; crust: crustaceans
243 (without copepods); eggs: fish eggs; erga: ergasilida copepods; harp: harpacticoids copepods;
244 naup: copepods nauplii; oith: oithonids copepods; pter: pteropods; salp: salp.

245 **3.2-Zooplankton interannual variations and relation with the** 246 **environmental trend**

247 The zooplankton community in the Bay of Marseille is dominated by calanoids (Fig 3A) which
248 represent more than 50% of the individuals sampled. The second most represented taxa were
249 appendicularians, oithonoids and crustaceans which represent with calanoids, on average, more
250 than 80% of the zooplankton community identified in this study. Obvious changes in relative
251 abundance of some species occurred over the observation period. The dominance of calanoids
252 seemed to have declined from more than 60% before 2012 to 50% after 2017, in contrast to the
253 relative abundance of crustaceans which almost doubled from 5 to 10% during the same period.
254 The changes in the relative abundances were mainly attributed by the diminution of copepod

255 calanoid and oithonoid absolute abundances (Fig 3B). More details concerning the patterns of
256 variation in the zooplankton community structure in species were observable on the interannual
257 series depicted at monthly scale (Fig 4). The abundances of bivalves, chaetognaths,
258 harpacticoids, crustaceans, pteropods, salps, appendicularians, fish eggs, and cnidarians seemed
259 to have increased during the study and breakpoints were detected for all these taxa (except for
260 cnidarians) in the last five years of the time series. The series of the two main copepod taxa
261 (calanoids and oithonoids), copepod nauplii and total zooplankton abundance showed a
262 diminution, and a breakpoint was detected for calanoids and oithonoids series at the end of 2012
263 (in November and September). Abundance estimations of ergasilida presented a breakpoint in
264 April 2007, resulting in an increase in abundance. Interannual variations of the sample scores
265 on the first MDS axis diminished (with a breakpoint detected in April 2014); this observation
266 was based mainly on the diminution of the copepod dominance while abundances of other
267 taxonomic groups such as chaetognaths and salps increased. The second axis highlighted the
268 increase in abundances of bivalves, harpacticoids and pteropods (breakpoint in October 2012).
269 The third axis represented the diminution of nauplii and increase of crustaceans abundance with
270 the breakpoint in April 2017. The smoothing of the first axis of the FPCA revealed that after a
271 displacement toward lower ESD values (between October 2009 - March 2012), the size spectra
272 shifted toward higher ESD after March 2012. No outstanding interannual variations of the
273 second PC were observable and no interannual structural change of the series was detected. The
274 biomass of the 1000 – 2000 μm size-fraction presented a breakpoint associated with a decrease
275 in September 2008. The three other zooplankton biomass size fractions decreased later, but no
276 breakpoints were detected.

277 **Fig 3. Year-to-year variations in the A) relative and B) absolute abundance of the 13 best**
278 **recognized zooplankton taxa.** Note that the graph is zoomed on the y values below 0.6 to
279 better see the species with low relative abundance. Abundances in the bottom panel are

280 expressed as number of individuals.m⁻³. The taxa are sorted by importance over the whole
281 zooplankton time series.

282 **Fig 4. Representations of the monthly interannual times series of the zooplankton**
283 **variables (black dots).** The red continuous (and dashed) lines correspond to the smoothing
284 (and its 95% confidence interval) by means of local regressions to describe the trends. The blue
285 lines correspond to the mean values of the series before and after a breakpoint date. For series
286 without blue lines no breakpoints were detected. Series of size-fractions biomasses, in mg.m⁻³,
287 (Biom 1000-2000, Biom 500-1000, Biom 300-500, Biom 200-300 μm), *taxa* abundances and
288 total zooplankton abundance, in individual.m⁻³, are log transformed (log₁₀(x+1)).

289 On the 12 models performed on the environmental data for the 2005-2020 period that have
290 converged, the DFA model with a diagonal and equal R matrix and displaying two trends was
291 considered as the best data model (see S3 file). The first trend (Fig 5A) was (a) positively
292 characterized by variations in S, concentrations of O₂, NH₄, NO₂, PO₄, POC, PON; and
293 abundances of bacteria (tot, HNA and LNA), *Cryptophyceae*, *Synechococcus*,
294 *Prochlorococcus*, pico-, nanoeukaryotes and microphytoplankton, and (b) negatively
295 characterized by variations in the size index of *Cryptophyceae* and nanoeukaryotes. This trend
296 decreased from 2005 to 2009, increased suddenly between 2011-2014 and decreased again
297 slowly until 2021. The second trend (Fig 5B) of this model was characterized by a sudden
298 increase between 2013 and 2014. Diatoms : dinoflagellates ratio was positively weighted while
299 size indices of bacteria, *Synechococcus*, *Prochlorococcus* and nanoeukaryotes were negatively
300 weighted. The fit of the data model to the environmental time series is represented in S3.

301 **Fig 5. The two trends depicted by the best DFA model (diagonal and equal R matrix and**
302 **two trends) on environmental data (2005-2020) and factor weights associated with each**
303 **trend.** Variables with positive weights are associated positively and depicted similar trends to
304 those shown in the left panels. Inversely, variables with negative weights displayed inverse

305 trends. Note that only the most significant factors (i.e. with weight higher than 0.2 in absolute
306 values) are represented. See Table 1 for abbreviations of factors.

307 All 12 models performed on the zooplankton data over the 2005-2020 period converged (see
308 S3 file). The model with two trends and a diagonal and unequal-type R matrix was the 'best'
309 data model deployed here. The first trend of this model peaked in 2007 and then decreased (Fig
310 6A). This trend displayed mainly positive variations of biomass series for every size fraction
311 and total zooplankton abundance, and negative variations of the second size structure indicator.
312 The second trend (Fig 6B) was characterized by a shift (decrease) between 2013 and 2014. This
313 trend allowed depiction of positive changes in the diversity community structure index (first
314 MDS axis) and negative changes in the size community structure index (first FPCA axis). In
315 Fig 6C, trend 2 of zooplankton (in red) and trend 2 of environment (in black, see Fig 5B) were
316 represented. Both trends presented common breakpoint in mid-2013. The fit of the data model
317 to the zooplankton time series is represented in S3.

318 **Fig 6. The two trends depicted by the best DFA model (diagonal and unequal R matrix)**
319 **on zooplankton data (biomass, size and diversity structure indices and total zooplankton**
320 **abundance series) between 2005-2020 and factor weights associated with each trend.**

321 Variables with positive weights are associated positively and depicted similar trends to those
322 shown in the left panels. Inversely, variables with negative weights displayed inverse trends.
323 A) and B) represent respectively the first and second zooplankton trends with their factor
324 weights. C) trend 2 of zooplankton (in red) and trend 2 of environment (in black, see Fig 5B)
325 are represented together. Vertical dotted blue line corresponds to common breakpoint detected
326 between both trends.

327 **3.3-Zooplankton seasonality and relationship between spring-** 328 **summer production and winter environment**

329 Most of the zooplankton series presented a clear seasonal pattern (Fig 7) but with different
330 shapes according to groups and size fractions. Seasonality assessments were significant (p -
331 values <0.05) for every variable except for the second axis of FPCA (see S4). The total
332 zooplankton abundance and biomass, the four-biomass size- fractions between 200 and 2000
333 μm , and the sample scores on the first axis of the MDS followed a similar seasonal pattern to
334 calanoids, oithonoids, ergasilida, bivalves, copepod nauplii and harpacticoids with their highest
335 abundance values in spring (April-May). The remaining zooplankton groups (appendicularians,
336 chaetognaths, cnidarians, crustaceans, pteropods, salps, fish eggs) and the two remaining MDS
337 axes seemed to reach their highest values during summer.

338 **Fig 7. Boxplot of the seasonal (monthly) pattern of the zooplankton time series.** When a
339 model (with one or two cycle) was significant, the average prediction was represented by means
340 of the red dashed line. The 95% confidence interval is represented by means of the blue lines.
341 Series of size-fractions biomasses, in $\text{mg}\cdot\text{m}^{-3}$, (Biom 1000-2000, Biom 500-1000, Biom 300-
342 500, Biom 200-300 μm , Total Biomass), *taxa* abundances and total zooplankton abundance, in
343 $\text{individual}\cdot\text{m}^{-3}$, are log transformed ($\log_{10}(x+1)$).

344 Fig 8 displays information regarding the patterns of change in the timing of the seasonal onset
345 the different taxonomic groups. A delay in the biomass size fraction between 200 and 1000 μm ,
346 total biomass and abundance, calanoids, ergasilida and appendicularians was observable while
347 salps tended to start their summer peak earlier. The other zooplankton groups did not present
348 such remarkable patterns.

349 **Fig 8. Level plots of the monthly interannual times series of the zooplankton variables.**
350 Circle colors correspond to the month value and the background color corresponds to smoothed
351 values with LOESS function over 30 equi-spaced points. Series of biomass size-fractions, in

352 mg of dry weight.m⁻³, (Biom 1000-2000, Biom 500-1000, Biom 300-500, Biom 200-300 μm,
353 Total Biomass), *taxa* abundances and total zooplankton abundance, in individuals.m⁻³, are log
354 transformed (log₁₀(x+1)). Year-to-year variations of the date of seasonal onset, considered as
355 20% of annually cumulative value for biomass and abundance time series, are represented by
356 the blue lines.

357 Fig 9 presents the results of the DFA performed under winter (January to March) environmental
358 conditions and the timing of zooplankton seasonal onset. This highlights a common decreasing
359 trend between the zooplankton phenology and the environmental compartment. This trend was
360 characterized with two plateaus between, 2009-2013 and 2015-2020. During the studied period
361 winter precipitations, NAO values, temperature, ratio Diatoms:Dinoflagellate, and abundances
362 of bacteria, LNA bacteria, *Cryptophyceas*, *Prochlorococcus* and Picophytoplankton increased. *A*
363 *contrario*, winter concentrations of oxygen, nitrite, phosphate, particulate organic matter
364 (POM), SPM and CHLA, abundances of HNA bacteria and sizes of bacteria (total, HNA and
365 LNA), *Cryptophyceas*, *Synechococcus*, *Prochlorococcus*, Picophytoplankton and
366 Nanoplankton decreased. To a lesser extent, MLD and microphytoplankton abundance were
367 positively associated with this trend (but not represented in the figure because of their low
368 weight 0.19<0.20 see S3). The interannual variations of winter environmental conditions were
369 associated with on one hand a later seasonal onset of biomass size fractions between 200 and
370 1000 μm, total biomass, and abundances of calanoids, ergasilida and appendicularians and, on
371 the other hand, an earlier seasonal onset of salps.

372 **Fig 9. Results of the best DFA model (diagonal and equal R matrix, one trend) performed**
373 **on environmental winter conditions and dates of zooplankton seasonal onset time series**
374 **(2005-2020).** A) The trend depicted by the DFA model. B) Baplot of the factors with the higher
375 weights (higher than 0.2 in absolute values) are represented. Green and red bars represent
376 respectively environmental and zooplankton series.

377 **4-Discussion**

378 **4.1-Seasonal and interannual variations of multiple zooplankton**

379 **indicators**

380 The seasonal patterns of the main zooplankton groups in the Bay of Marseille during the time
381 series are consistent with zooplankton successions observed in Mediterranean coastal areas
382 [5,27,51–54], with a zooplankton community dominated by copepods in response to the spring
383 phytoplankton blooms and a second late summer - fall peak of abundance. In the Gulf of Lion,
384 phytoplankton-zooplankton peaks are associated for both periods with strong grazing activity
385 [14]. The second peak is associated with higher diversity indices (as shown in Fig.7 and 8)
386 linked to a relative diminution of the copepod contribution (mainly calanoids and oithonoids)
387 and the appearance of other taxonomic groups (either herbivorous taxa feeding on small size
388 phytoplankton, such as salps and pteropods, or carnivorous taxa, such as chaetognaths,
389 crustaceans and cnidarians), a general pattern already described in the NW Mediterranean Sea
390 [11].

391 Our results showed different interannual patterns among the size-fraction biomass dynamics
392 (see Fig. 4). The sudden decline in 2008 for the largest size-fraction (1000-2000 μm) was not
393 simultaneously observed for the three other fractions (between 200 and 1000 μm) which
394 decreased between 2 and 4 years later. No major change in the community diversity was
395 observed in 2008, while the diminution of the larger size fraction biomass was accompanied by
396 a shift in the size structure of the zooplankton community. Previous studies in the Bay of
397 Marseille have shown that the taxonomic assemblages are not the same in the four size fractions
398 [55,56], impacting differently the biomass dynamics of each size fraction. The size-fractioned
399 approach enabled us to highlight these differences between the size fraction biomass dynamics

400 that would have gone unnoticed if considering the whole biomass. This revealed the strong link
401 between the biomass size-fraction dynamic and community size structure.

402 Our results are also consistent with the zooplankton dynamics of the Bay of Calvi [27] and the
403 Bay of Villefranche-sur-Mer [54] during the same decade. The main changes in the zooplankton
404 community in the Bay of Marseille observed between 2012 and 2014 (see Fig. 4 & 6) appear
405 to have occurred earlier than similar variations in the whole mesozooplankton community
406 observed after 2015 at Villefranche-sur-Mer [54], where crustaceans (including copepods in
407 their study) showed a diminution of abundance and a lower size spectrum slope (mainly due to
408 the loss of small copepods). In their analysis of multiple time series in the Mediterranean Sea,
409 Berline et al. [5] did not find any common zooplankton interannual patterns at basin scale.
410 Nevertheless, our results and those at Villefranche-sur-mer and Calvi suggest that the coastal
411 regions of the Ligurian Sea might be similarly impacted by the environmental changes and by
412 their connections through the Ligurian current [57]. As the re-analysis of time series with recent
413 data proved that some environmental-biological processes relationships may break down [58].
414 Reanalyses of zooplankton time series in the Mediterranean Sea with longer time series are
415 required to assess some large-scale processes.

416 The different community level indicators (i.e. size-fraction biomasses, total zooplankton
417 abundance, size- and diversity- structure) used in our study highlighted shifts occurring in
418 different years (Fig. 4 & 6) denoting structural changes that would not have been perceived by
419 more aggregated variables (e.g. total abundance or total biomass). In 2014 the assemblage
420 composition from image analysis was sufficient to explain the shift. However, a finer taxonomic
421 reanalysis would certainly be necessary to understand the 2008 shift potentially due to changes
422 within the calanoid group, a group with high diversity in species composition, size distribution
423 and trophic behavior [59,60]. In addition, such a more detailed taxonomic identification, up to
424 separation of adult and copepodite stages, could help to better interpret the fine changes in size

425 spectrum, highly sensitive to the underlying assemblage compositions and their associated size
426 distribution.

427 Overall the multiple indicator approach used in our study helped us to better characterize and
428 understand the zooplankton community dynamic. Pitois et al. [2] also advocated a multi-
429 indicator approach as necessary for describing zooplankton structural changes.

430 **4.2- Variations of the environmental conditions and link with** 431 **zooplankton**

432 In the present study, we aimed to understand the observed zooplankton variations within an
433 ecosystemic framework at the study site (as shown in Fig 5) including changes in the abiotic
434 conditions and in the lower trophic levels (micro- nano- pico-plankton). We described multiple
435 environmental trends:

- 436 - Higher values of salinity and oxygen between 2005 and 2007 (Fig 5, trend 1). This
437 anomaly can be interpreted as the signature of stronger offshore deep-water inflows
438 during this period. By analyzing satellite images in those years, Mayot et al. [61]
439 highlighted particularly high phytoplankton productivity induced by strong deep water
440 convection events occurring over a broad area in the Provencal basin with effects
441 extending to surrounding coastal areas, including the Bay of Marseille.
- 442 - The reduction in nutrients and particulate matter inputs observed in our time series (Fig
443 5, trend 1) is consistent with observations already made in the Bay of Marseille, and
444 appears to be a general trend in French Mediterranean coastal waters [62,63]. The
445 physical and chemical characteristics of the Bay of Marseille might have been impacted
446 by the diminution of the Rhône nutrient inputs in the Gulf of Lion [64] and/or by the
447 proximity to the Marseille sewage treatment plant where the treatment efficiency has
448 improved since 2008 [32,65]. While ammonium and phosphate decreased, nitrate

449 concentration was stabilized (and even presented a slight increase in the second part of
450 the study, see S3 file).

451 - As autotrophic planktonic groups show preferences in nutrient uptake [66], the
452 variations in the stoichiometry of nutrient sources and their concentrations may have
453 affected their distribution. Our observations evidenced changes in size and abundance
454 of the micro-, nano-, pico-plankton in 2013 after the strong decrease in nutrient
455 concentrations which were concomitant with changes in the mesozooplankton
456 community structure (Fig 5B, Fig 6B and Fig 6C). This supports the hypothesis of a
457 regime shift in the whole pelagic food web through bottom-up cascading effects [67,68],
458 similarly to those described in Rietkerk et al. [69]. The concomitant decline of calanoid
459 copepods and increase in appendicularians and salps represented an indicator of such
460 change in the zooplankton community. Because appendicularians and salps can feed on
461 smaller particles, the trophic competition with calanoid copepods (feeding on larger
462 particles) seemed to be reduced [70,71]. When copepods are unable to feed on large
463 microphytoplankton, they often switch to microzooplankton [72,73] resulting in a
464 higher trophic level of copepods [67]. The hypothesis of such a relationship between
465 the phytoplankton size and zooplankton assemblages has been suggested in the NW
466 Mediterranean Sea [54,74]. These changes in the Bay of Marseille were accompanied
467 with the appearance of predators such as chaetognaths or cnidarians. In the Catalan Sea,
468 the predation impact of chaetognaths on the standing stock of copepod was low, but
469 chaetognaths can exert a high level of predation on specific copepod species and stages
470 under food-limited conditions [75]. A species level taxonomy would help to quantify
471 the top-down pressure of predators on copepods species dynamics.

472 In parallel, by analyzing the winter environmental conditions, we observed a relationship
473 between NAO, precipitation, temperature, and zooplankton phenology (Fig 9). Although at

474 Mediterranean scale no relationship was found between NAO and zooplankton by Berline et al.
475 [5], several studies suggested that winter conditions at NW Mediterranean Sea regional scale
476 (inducing strong variation in the NAO index) impacted the following zooplankton spring peak
477 [4,27,28], as shown by our results (and discussed in the previous section). Since 2014, winter
478 deep convection (associated with climatic forcing NAO) declined in the NW Mediterranean
479 Sea causing a stratification and water warming [76]. This was concomitant with the increase of
480 winter temperature, NAO and precipitation in the Bay of Marseille, and (i) a later seasonal onset
481 of the 200-1000 μm zooplankton biomass, copepods (calanoids and ergasilida),
482 appendicularians, total zooplankton (ii) an earlier seasonal onset of salps. Therefore, we cannot
483 exclude the hypothesis that winter large-scale forcing impacted the coastal zooplankton
484 dynamics in the Bay of Marseille in the 2010s.

485 **4.3-Implications of the variations in the pelagic ecosystem**

486 The conceptual schema, Fig 10, summarizes the interannual changes analyzed in the present
487 paper concerning the environment of the Bay of Marseille and its mesozooplankton community.
488 The results of the Bay of Marseille time series contribute to the documentation of the alterations
489 in the Mediterranean pelagic ecosystem [77], particularly changes occurring in the Gulf of Lion.
490 Espinasse et al. [17], on the basis of a large-scale survey in winter and spring, defined three
491 zooplankton habitats in the Gulf of Lion: the continental shelf, the Rhone influence zone and
492 the Occitan littoral zone. They found that the zooplankton habitat in the BoM presented the
493 same environmental and biological characteristics as most of the Gulf of Lion continental shelf.
494 Therefore, the Bay of Marseille time series can be considered as a sentinel zone for monitoring
495 environmental effects from the open sea as well as the coastal area.

496 **Fig 10. Summary of our main results by means of the revisited Ramon Margalef mandala**
497 **[78].** In the schema, the significant interannual changes of the zooplankton community and

498 environmental parameters are represented along the timeline materialized by the black arrow.
499 The variables around the green square exerted a direct or indirect bottom-up control on the
500 interannual zooplankton community dynamic: (1) Nutrients stoichiometry, (2) POM and
501 nutrients quantity, (3) Micro-, Nano-, Pico- plankton size, (4) Winter conditions. The taxonomic
502 groups within in the central square highlight the main variations of the zooplankton community
503 composition. The variations in the zooplankton community traits are represented around the red
504 square: (5) Biomass and abundance, (6) Size structure and diversity, (7) Seasonal onset. Finally,
505 the implications for planktivorous fish are represented within the blue squares: (8) Quantity of
506 food variation, (9) Preferred prey variation, (10) Match-Mismatch.

507 The observed sudden diminution of the larger mesozooplankton size fraction biomass (shown
508 in Fig 4) coincided with the shift in fish body condition at Gulf of Lion scale evidenced in 2008
509 [20] and with observed changes in the diets of small pelagic fishes [19]. This supports the
510 hypothesis of a bottom-up control of the pelagic food chain up to the planktivorous fishes in
511 the Gulf of Lion [24,64], as shown in other areas in the Mediterranean Sea [79,80].

512 By taking into account indicators related to the zooplankton populations seasonal onset, we
513 show that the process of match/mismatch with small pelagic fish [81] may be a process at work
514 in the Gulf of Lion. An increased mismatch between the spring peak of zooplankton biomass
515 (mainly calanoids) and the growth phase of small pelagic fish [82-84] could certainly explain
516 their body condition. In their experimental study, Queiros et al. [85], showed that sardine can
517 display adaptative phenotypic plasticity to food condition changes. Under lower food quantity
518 and quality conditions, the smallest phenotypes experienced lower mortality by starvation than
519 the larger ones during the critical post-reproductive period (i.e. at the end of winter). In this
520 context, a delay in the availability of these preferred fish prey might favor smaller fish
521 phenotypes. In addition, the zooplankton biochemical composition and energy content may
522 vary seasonally [56,86] due to the reorganization of different zooplankton assemblages. Further

523 investigations of the interannual variations of the mesozooplankton quality, both in species
524 composition and biochemical content, are needed to improve our understanding of changes in
525 the trophic environment of the small pelagic fishes.

526 **Supporting information**

527 **S1 File. Supplementary information on environmental and zooplankton monitoring**

528 **S2 File. Performance of ParticleTrieur software for the detection of individuals.**

529 **S3 File. Summary of the results of the Dynamic Factor Analysis.**

530 **S4 Table. Seasonality assessment.** Summary of the statistics of the sinusoidal model for
531 zooplankton seasonality assessment. In bold, significant seasonal patterns (p-value <0.05).

532 **Acknowledgements**

533 The zooplankton time series was initiated in 2002 by F. Carlotti and was linked with the on-
534 going SOMLIT monitoring program. The authors acknowledge all participants in the Bay of
535 Marseille SOMLIT monitoring program: Patrick Raimbault as PI of the program, Michel Lafont
536 for the regular sampling of physical and biogeochemical parameters, and the crew of the R.V.
537 Antedon II. The regular sampling of zooplankton was carried out before 2012 mainly by
538 F. Carlotti's students as part of their PhD or MSc work, V. Riandey, E. Dieval, A. Nowaczyk,
539 K. Morsly, N. Neffati, A. Dron, S. Martini, then after 2012, mainly by L. Guilloux (Research
540 Engineer CNRS), sometimes supported by PhD students K. Donoso, C-T Chen and T Garcia.
541 We would like to thank all of them for their contribution to this sampling effort. We thank P.
542 Raimbault, N. Garcia and M. Lafont for making available the physical and biogeochemical
543 data, and V. Cornet, S. Boussabat and K. Leblanc for processing the phytoplankton samples
544 whose data are used. Chemical and biological sample treatments benefited from the
545 Mediterranean Institute of Oceanography platforms (PACEM for chemical analyses and MIM

546 for microscopy and imagery). Flow cytometry analyses have been performed, for SOMLIT, at
547 the BioPIC platform (Biology Platform of Imaging and flow Cytometry) of the Oceanology
548 Observatory of Banyuls-sur-Mer (OOB) by Christophe Salmeron and David Pecqueur, in
549 collaboration with G. Grégori (MIO, Cytometry manager for SOMLIT). The zooplankton scan
550 treatment used the ParticleTrieur Software for images classification. We thank R. Marchant
551 (researcher, James Cook University), software designer, for his support in the use of the
552 Software, as well as T. Duong Quoc, postdoctoral fellow, in the frame of the on-going RAP-
553 Med project (<https://rapmed.osupytheas.fr/>, funded by Aix-Marseille University ITEM project
554 (PIs T De Garidel and C Chevalier). We thank M. Peraud, MSc student, in the frame of RAP-
555 Med ITEM, for her contributions to the design of the learning set. This work contributes to the
556 valorization of observational time series strategy and to the understanding of pelagic ecosystem
557 functioning developed respectively by the national research organisation ILICO and by
558 previous research in the frame of the CNRS-INSU MISTRALS MERMEX program
559 (subprograms IPP and MERITE). Thanks to W. Podlejski for his comments on the manuscript.
560 Thanks are also addressed to Michael Paul, native speaker, for English proofreading.

561 Bibliography

- 562 1. Beaugrand G. Monitoring pelagic ecosystems using plankton indicators. *ICES J Mar Sci.* 2005;62(3):333-8.
- 563 2. Pitois SG, Graves CA, Close H, Lynam C, Scott J, Tilbury J, et al. A first approach to build and test the
564 Copepod Mean Size and Total Abundance (CMSTA) ecological indicator using in-situ size measurements
565 from the Plankton Imager (PI). *Ecol Indic.* 2021;123:107307.
- 566 3. Planque B, Taylor AH. Long-term changes in zooplankton and the climate of the North Atlantic. *ICES J Mar*
567 *Sci.* 1998;55(4):644-54.
- 568 4. García-Comas C, Stemmann L, Ibanez F, Berline L, Mazzocchi MG, Gasparini S, et al. Zooplankton long-term
569 changes in the NW Mediterranean Sea: Decadal periodicity forced by winter hydrographic conditions
570 related to large-scale atmospheric changes? *J Mar Syst.* 2011;87(3):216-26.
- 571 5. Berline L, Siokou-Frangou I, Marasović I, Vidjak O, Fernández de Puelles ML, Mazzocchi MG, et al.
572 Intercomparison of six Mediterranean zooplankton time series. *Prog Oceanogr.* 2012;97-100:76-91.
- 573 6. Fanjul A, Villate F, Uriarte I, Iriarte A, Atkinson A, Cook K. Zooplankton variability at four monitoring sites of
574 the Northeast Atlantic Shelves differing in latitude and trophic status. *J Plankton Res.* 2017;39(6):891-909.

- 575 7. Hays GC, Richardson AJ, Robinson C. Climate change and marine plankton. *Trends Ecol Evol.*
576 2005;20(6):337-44.
- 577 8. Mackas DL, Greve W, Edwards M, Chiba S, Tadokoro K, Eloire D, et al. Changing zooplankton seasonality in
578 a changing ocean: Comparing time series of zooplankton phenology. *Prog Oceanogr.* 2012;97-100:31-62.
- 579 9. Pagano M, Gaudy R, Thibault D, Lochet F. Vertical Migrations and Feeding Rhythms of Mesozooplanktonic
580 Organisms in the Rhône River Plume Area (North-west Mediterranean Sea). *Estuar Coast Shelf Sci.*
581 1993;37(3):251-69.
- 582 10. Razouls C, Kouwenberg J. Spatial distribution and seasonal variation of mesozooplankton biomass in the
583 Gulf of Lions (northwestern Mediterranean). *Oceanol Acta.* 1993;(16):393-401.
- 584 11. Champalbert G. Characteristics of zooplankton standing stock and communities in the Western
585 Mediterranean Sea: Relations to hydrology. *Sci Mar.* 1996;60:97-113.
- 586 12. Gaudy R, Champalbert G. Space and time variations in zooplankton distribution south of Marseilles.
587 *Oceanol Acta.* 1998;21(6):793-802.
- 588 13. Plounevez S, Champalbert G. Diet, feeding behaviour and trophic activity of the anchovy (*Engraulis*
589 *encrasicolus* L.) in the Gulf of Lions (Mediterranean Sea). *Oceanol Acta.* 2000;23(2):175-92.
- 590 14. Gaudy R, Youssara F, Diaz F, Raimbault P. Biomass, metabolism and nutrition of zooplankton in the Gulf of
591 Lions (NW Mediterranean). *Oceanol Acta.* 2003;26(4):357-72.
- 592 15. Raimbault P, Durrieu de Madron X. Research activities in the Gulf of Lion (NW Mediterranean) within the
593 1997–2001 PNEC project. *Oceanol Acta.* 2003;26(4):291-8.
- 594 16. Palomera I, Olivar MP, Salat J, Sabatés A, Coll M, García A, et al. Small pelagic fish in the NW
595 Mediterranean Sea: An ecological review. *Prog Oceanogr.* 2007;74(2-3):377-96.
- 596 17. Espinasse B, Carlotti F, Zhou M, Devenon JL. Defining zooplankton habitats in the Gulf of Lion (NW
597 Mediterranean Sea) using size structure and environmental conditions. *Mar Ecol Prog Ser.* 2014;506:31-46.
- 598 18. Saiz E, Sabatés A, Gili JM. The Zooplankton. In: Goffredo S, Dubinsky Z, éditeurs. *The Mediterranean Sea.*
599 Dordrecht: Springer Netherlands; 2014 . p. 183-211. [https://link.springer.com/10.1007/978-94-007-6704-](https://link.springer.com/10.1007/978-94-007-6704-1_11)
600 [1_11](https://link.springer.com/10.1007/978-94-007-6704-1_11)
- 601 19. Bourg BL. Trophic niche overlap of sprat and commercial small pelagic teleosts in the Gulf of Lions (NW
602 Mediterranean Sea). *J Sea Res.* 2015;9.
- 603 20. Van Beveren E, Bonhommeau S, Fromentin JM, Bigot JL, Bourdeix JH, Brosset P, et al. Rapid changes in
604 growth, condition, size and age of small pelagic fish in the Mediterranean. *Mar Biol.* 2014;161(8):1809-22.
- 605 21. Bănaru D, Mellon-Duval C, Roos D, Bigot JL, Souplet A, Jadaud A, et al. Trophic structure in the Gulf of Lions
606 marine ecosystem (north-western Mediterranean Sea) and fishing impacts. *J Mar Syst.*
607 2013;111-112:45-68.
- 608 22. Van Beveren E, Fromentin JM, Bonhommeau S, Nieblas AE, Metral L, Brisset B, et al. Predator–prey
609 interactions in the face of management regulations: changes in Mediterranean small pelagic species are
610 not due to increased tuna predation. *Can J Fish Aquat Sci.* 2017;74(9):1422-30.
- 611 23. GFCM. Scientific Advisory Committee on Fisheries (SAC) Working Group on Stock Assessment of Small
612 Pelagic species (WGSASP). 2017.
- 613 24. Saraux C, Van Beveren E, Brosset P, Queiros Q, Bourdeix JH, Dutto G, et al. Small pelagic fish dynamics: A
614 review of mechanisms in the Gulf of Lions. *Deep Sea Res Part II Top Stud Oceanogr.* 2019;159:52-61.

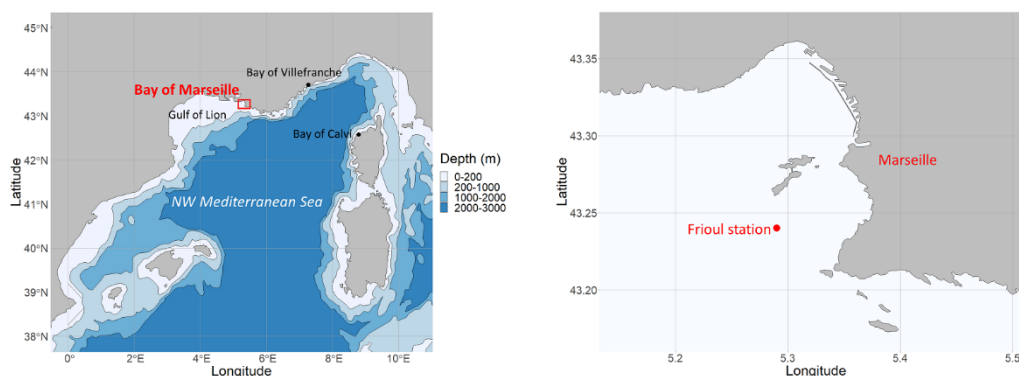
- 615 25. Brosset P, Le Bourg B, Costalago D, Bănaru D, Van Beveren E, Bourdeix J, et al. Linking small pelagic dietary
616 shifts with ecosystem changes in the Gulf of Lions. *Mar Ecol Prog Ser.* 2016;554:157-71.
- 617 26. Serranito B, Jamet JL, Rossi N, Jamet D. Decadal shifts of coastal microphytoplankton communities in a
618 semi-enclosed bay of NW Mediterranean Sea subjected to multiple stresses. *Estuar Coast Shelf Sci.*
619 2019;224:171-86.
- 620 27. Fullgrabe L, Grosjean P, Gobert S, Lejeune P, Leduc M, Engels G, et al. Zooplankton dynamics in a changing
621 environment: A 13-year survey in the northwestern Mediterranean Sea. *Mar Environ Res.*
622 2020;159:104962.
- 623 28. Fernández de Puellas ML, Alemany F, Jansá J. Zooplankton time-series in the Balearic Sea (Western
624 Mediterranean): Variability during the decade 1994–2003. *Prog Oceanogr.* 2007;74(2):329-54.
- 625 29. Millot C. Wind induced upwellings in the gulf of lions. *Oceanol Acta.* 1979;2(3):261-74.
- 626 30. Pinazo C, Frayssé M, Doglioli A, Faure VM, Pairaud I, Petrenko A, et al. MASSILIA: Modélisation de la baie
627 de MARSeILLE : Influence des apports Anthropiques de la métropole sur l'écosystème marin. 2013 ;
628 <https://archimer.ifremer.fr/doc/00145/25592/>
- 629 31. Millot C. Circulation in the Western Mediterranean Sea. *J Mar Syst.* 1999;20(1):423-42.
- 630 32. Millet B, Pinazo C, Banaru D, Pagès R, Guiart P, Pairaud I. Unexpected spatial impact of treatment plant
631 discharges induced by episodic hydrodynamic events: Modelling Lagrangian transport of fine particles by
632 Northern Current intrusions in the bays of Marseille (France). *PLOS ONE.* 2018;13(4):e0195257.
- 633 33. Gregoire D. France Geojson. 2018. <https://github.com/gregoire david/france-geojson>
- 634 34. Martin-Vide J, Lopez-Bustins JA. The Western Mediterranean Oscillation and rainfall in the Iberian
635 Peninsula. *Int J Climatol.* 2006;26(11):1455-75.
- 636 35. Quéguiner B, Carlotti F, Leblanc K, Salter I, Golbol M, Guilloux L, et al. Mistrals/Specimed Project: Seasonal
637 And Interannual Variability Of Plankton Communities Structure And Biogeochemical Cycles In North-
638 Western Mediterranean. In 2013.
- 639 36. Phytobs. PHYTOBS dataset - French National Service of Observation for Phytoplankton in coastal waters.
640 SEANOE; 2021. <https://www.seanoe.org/data/00740/85178/>
- 641 37. Gorsky G, Ohman MD, Picheral M, Gasparini S, Stemann L, Romagnan JB, et al. Digital zooplankton image
642 analysis using the ZooScan integrated system. *J Plankton Res.* 2010;32(3):285-303.
- 643 38. Jennings BR, Parslow K, Ottewill RH. Particle size measurement: the equivalent spherical diameter. *Proc R*
644 *Soc Lond Math Phys Sci.* 1988;419(1856):137-49.
- 645 49. Marchant R, Tetard M, Pratiwi A, Adebayo M, de Garidel-Thoron T. Automated analysis of foraminifera
646 fossil records by image classification using a convolutional neural network. *J Micropalaeontology.*
647 2020;39(2):183-202.
- 648 40. R Core Team. R: A Language and Environment for Statistical Computing. Vienna, Austria: R Foundation for
649 Statistical Computing; 2022. <https://www.R-project.org/>
- 650 41. Tukey JW (John W. Exploratory data analysis [Internet]. Reading, Mass. : Addison-Wesley Pub. Co.; 1977.
651 714 p. http://archive.org/details/exploratorydataa0000tukey_7616
- 652 42. Nerini D, Ghattas B. Classifying densities using functional regression trees: Applications in oceanology.
653 *Comput Stat Data Anal.* 2007;51(10):4984-93.

- 654 43. Ramsay JO, Hooker G, Graves S. Introduction to Functional Data Analysis. In: Ramsay J, Hooker G, Graves S,
655 éditeurs. *Functional Data Analysis with R and MATLAB* [Internet]. New York, NY: Springer; 2009. p. 1-19.
656 (Use R). https://doi.org/10.1007/978-0-387-98185-7_1
- 657 44. Pauthenet E, Roquet F, Madec G, Nerini D. A Linear Decomposition of the Southern Ocean Thermohaline
658 Structure. *J Phys Oceanogr*. 2017;47(1):29-47.
- 659 45. Dixon P. VEGAN, a package of R functions for community ecology. *J Veg Sci*. 2003;14(6):927-30.
- 660 46. Audigier V, Husson F, Josse J. Multiple imputation for continuous variables using a Bayesian principal
661 component analysis. arXiv; 2015.<http://arxiv.org/abs/1401.5747>
- 662 47. Zeileis A, Leisch F, Hornik K, Kleiber C. strucchange: An R Package for Testing for Structural Change in
663 Linear Regression Models. *J Stat Softw*. 2002;7:1-38.
- 664 48. Greve W, Lange U, Reiners F, Nast J. Predicting the seasonality of North Sea zooplankton. *Senckenberg
665 Maritima*. 2001;31(2):263-8.
- 666 49. Zuur AF, Fryer RJ, Jolliffe IT, Dekker R, Beukema JJ. Estimating common trends in multivariate time series
667 using dynamic factor analysis. *Environmetrics*. 2003;14(7):665-85.
- 668 50. Holmes E E, Ward E J, Wills K. MARSS: Multivariate Autoregressive State-space Models for Analyzing Time-
669 series Data. *R J*. 2012;4(1):11.
- 670 51. Fernández de Puellas ML, Macias V, Vicente L, Molinero JC. Seasonal spatial pattern and community
671 structure of zooplankton in waters off the Balears archipelago (Central Western Mediterranean). *J Mar
672 Syst*. 2014;138:82-94.
- 673 52. Romagnan JB, Legendre L, Guidi L, Jamet JL, Jamet D, Mousseau L, et al. Comprehensive Model of Annual
674 Plankton Succession Based on the Whole-Plankton Time Series Approach. *PLOS ONE*.
675 2015;10(3):e0119219.
- 676 53. García-Martínez M del C, Vargas-Yáñez M, Moya F, Santiago R, Reul A, Muñoz M, et al. Spatial and
677 Temporal Long-Term Patterns of Phyto and Zooplankton in the W-Mediterranean: RADMED Project.
678 *Water*. 2019;11(3):534.
- 679 54. Feuilloley G, Fromentin J marc, Saraux C, Irsson JO, Jalabert L, Stemmann L. Temporal fluctuations in
680 zooplankton size, abundance, and taxonomic composition since 1995 in the North Western Mediterranean
681 Sea. *ICES J Mar Sci*. 2021; <https://hal.archives-ouvertes.fr/hal-03374991>
- 682 55. Bănaru D, Carlotti F, Barani A, Grégori G, Neffati N, Harmelin-Vivien M. Seasonal variation of stable isotope
683 ratios of size-fractionated zooplankton in the Bay of Marseille (NW Mediterranean Sea). *J Plankton Res*.
684 2014;36(1):145-56.
- 685 56. Chen CT, Bănaru D, Carlotti F, Faucheux M, Harmelin-Vivien M. Seasonal variation in biochemical and
686 energy content of size-fractionated zooplankton in the Bay of Marseille (North-Western Mediterranean
687 Sea). *J Mar Syst*. 2019;199:103223.
- 688 57. Berline L, Rammou AM, Doglioli A, Molcard A, Petrenko A. A Connectivity-Based Eco-Regionalization
689 Method of the Mediterranean Sea. *PLOS ONE*. 2014;9(11):e111978.
- 690 58. Myers RA. When Do Environment–recruitment Correlations Work? *Rev Fish Biol Fish*. 1998;8(3):285-305.
- 691 59. Kleppel G. On the diets of calanoid copepods. *Mar Ecol Prog Ser*. 1993;99:183-95.
- 692 60. Beaugrand G, Reid P, Ibañez F, Planque B. Biodiversity of North Atlantic and North Sea calanoid copepods.
693 *Mar Ecol Prog Ser*. 2000;204:299-303.

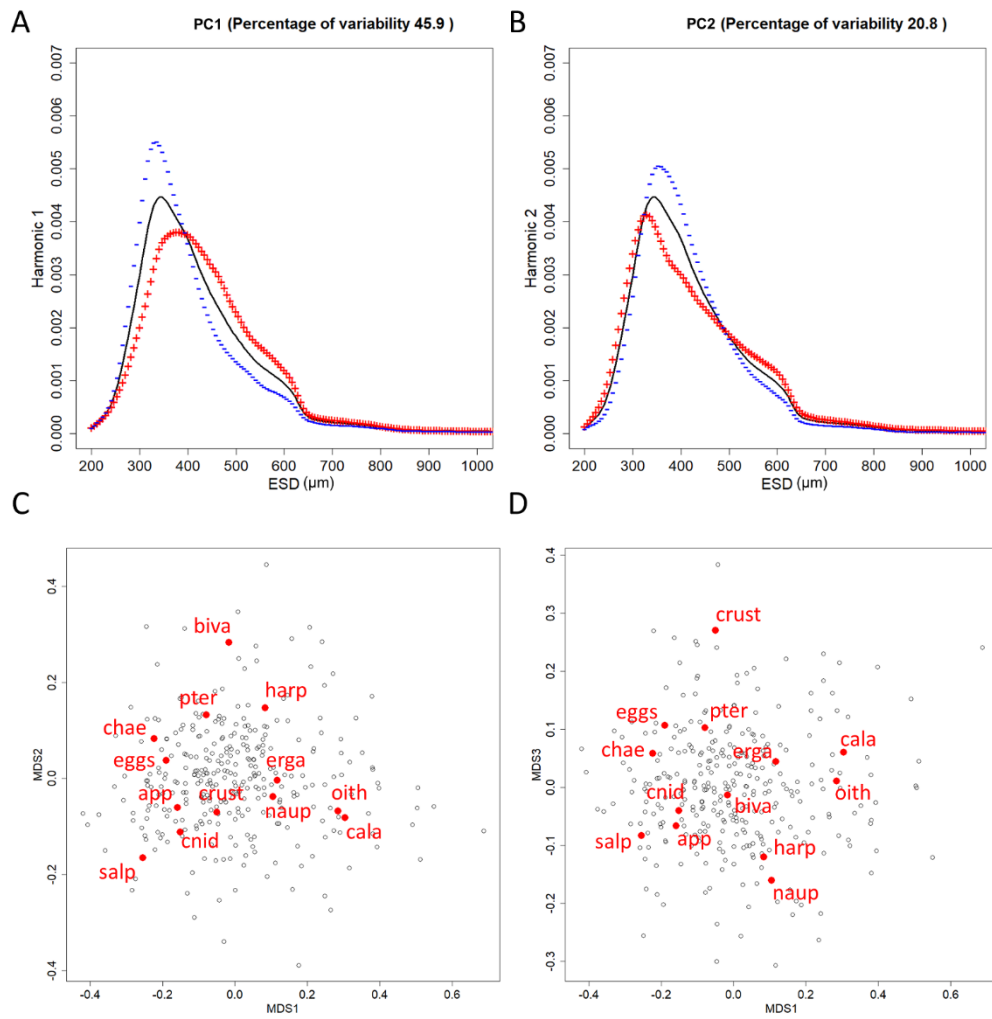
- 694 61. Mayot N, D'Ortenzio F, Uitz J, Gentili B, Ras J, Vellucci V, et al. Influence of the Phytoplankton Community
695 Structure on the Spring and Annual Primary Production in the Northwestern Mediterranean Sea. *J*
696 *Geophys Res Oceans*. 2017;122(12):9918-36.
- 697 62. Lheureux A, Savoye N, Amo YD, Goberville E, Bozec Y, Breton E, et al. Bi-decadal variability in physico-
698 biogeochemical characteristics of temperate coastal ecosystems: from large-scale to local drivers. *Mar Ecol*
699 *Prog Ser*. 2021;660:19-35.
- 700 63. Goberville E, Beaugrand G, Sautour B, Tréguer P, Team S. Climate-driven changes in coastal marine
701 systems of western Europe. *Mar Ecol Prog Ser*. 2010;408:129-48.
- 702 64. Feuilloley G, Fromentin JM, Stemann L, Demarcq H, Estournel C, Saraux C. Concomitant changes in the
703 environment and small pelagic fish community of the Gulf of Lions. *Prog Oceanogr*. 2020;186:102375.
- 704 65. Raimbault P, Boudouresque CF, Bănaru D, Jacquet S, Thibault D, Vincente N, et al. Chapitre 7 : Le milieu
705 marin autour de Marseille. In: Curt T, Guiot J, Mazurek H, éditeurs. Marseille et l'environnement Bilan,
706 qualité et enjeux : Le développement durable d'une grande ville littorale face au changement climatique.
707 Aix-en-Provence: Presses universitaires de Provence; 2021. p. 171-219. (Hors collection).
708 <http://books.openedition.org/pup/41463>
- 709 66. Probyn TA, Painting SJ. Nitrogen uptake by size-fractionated phytoplankton populations in Antarctic
710 surface waters. *Limnol Oceanogr*. 1985;30(6):1327-32.
- 711 67. Sommer U, Stibor H, Katechakis A, Sommer F, Hansen T. Pelagic food web configurations at different levels
712 of nutrient richness and their implications for the ratio fish production:primary production. In: Vadstein O,
713 Olsen Y, éditeurs. Sustainable Increase of Marine Harvesting: Fundamental Mechanisms and New
714 Concepts: Proceedings of the 1st Maricult Conference held in Trondheim, Norway, 25–28 June 2000.
715 Dordrecht: Springer Netherlands; 2002. p. 11-20. https://doi.org/10.1007/978-94-017-3190-4_2
- 716 68. Stibor H, Vadstein O, Diehl S, Gelzleichter A, Hansen T, Hantzsche F, et al. Copepods act as a switch
717 between alternative trophic cascades in marine pelagic food webs. *Ecol Lett*. 2004;7(4):321-8.
- 718 69. Rietkerk M, Dekker SC, de Ruiter PC, van de Koppel J. Self-Organized Patchiness and Catastrophic Shifts in
719 Ecosystems. *Science*. 2004;305(5692):1926-9.
- 720 70. Flood PR, Deibel D, Morris CC. Filtration of colloidal melanin from sea water by planktonic tunicates.
721 *Nature*. 1992;355(6361):630-2.
- 722 71. Katechakis A, Stibor H, Sommer U, Hansen T. Feeding selectivities and food niche separation of *Acartia*
723 *clausi*, *Penilia avirostris* (Crustacea) and *Doliolum denticulatum* (Thaliacea) in Blanes Bay (Catalan Sea, NW
724 Mediterranean). *J Plankton Res*. 2004;26(6):589-603.
- 725 72. Stoecker DK, Capuzzo JM. Predation on Protozoa: its importance to zooplankton. *J Plankton Res*.
726 1990;12(5):891-908.
- 727 73. Irigoien X, Head RN, Harris RP, Cummings D, Harbour D, Meyer-Harms B. Feeding selectivity and egg
728 production of *Calanus helgolandicus* in the English Channel. *Limnol Oceanogr*. 2000;45(1):44-54.
- 729 74. Calbet A, Garrido S, Saiz E, Alcaraz M, Duarte CM. Annual Zooplankton Succession in Coastal NW
730 Mediterranean Waters: The Importance of the Smaller Size Fractions. *J Plankton Res*. 2001;23(3):319-31.
- 731 75. Duró A, Saiz E. Distribution and trophic ecology of chaetognaths in the western Mediterranean in relation
732 to an inshore–offshore gradient. *J Plankton Res*. 2000;22(2):339-61.
- 733 76. Margirier F, Testor P, Heslop E, Mallil K, Bosse A, Houpert L, et al. Abrupt warming and salinification of
734 intermediate waters interplays with decline of deep convection in the Northwestern Mediterranean Sea.
735 *Sci Rep*. 2020;10(1):20923.

- 736 77. Durrieu de Madron X, Guieu C, Sempéré R, Conan P, Cossa D, D’Ortenzio F, et al. Marine ecosystems’
737 responses to climatic and anthropogenic forcings in the Mediterranean. *Prog Oceanogr.*
738 2011;91(2):97-166.
- 739 78. Glibert PM. Margalef revisited: A new phytoplankton mandala incorporating twelve dimensions, including
740 nutritional physiology. *Harmful Algae.* 2016;55:25-30.
- 741 79. Macias D, Garcia-Gorriz E, Piroddi C, Stips A. Biogeochemical control of marine productivity in the
742 Mediterranean Sea during the last 50 years. *Glob Biogeochem Cycles.* 2014;28(8):897-907.
- 743 80. Piroddi C, Coll M, Liqueste C, Macias D, Greer K, Buszowski J, et al. Historical changes of the Mediterranean
744 Sea ecosystem: modelling the role and impact of primary productivity and fisheries changes over time. *Sci*
745 *Rep.* 2017;7(1):44491.
- 746 81. Cushing DH. Plankton Production and Year-class Strength in Fish Populations: an Update of the
747 Match/Mismatch Hypothesis. In: Blaxter JHS, Southward AJ, éditeurs. *Advances in Marine Biology.*
748 Academic Press; 1990. p. 249-93. <https://www.sciencedirect.com/science/article/pii/S0065288108602023>
- 749 82. Costalago D, Palomera I. Feeding of European pilchard (*Sardina pilchardus*) in the northwestern
750 Mediterranean: from late larvae to adults. *Sci Mar.* 2014;78(1):41-54.
- 751 83. Nikolioudakis N, Isari S, Somarakis S. Trophodynamics of anchovy in a non-upwelling system: direct
752 comparison with sardine. *Mar Ecol Prog Ser.* 2014;500:215-29.
- 753 84. Chen CT, Carlotti F, Harmelin-Vivien M, Guilloux L, Bănaru D. Temporal variation in prey selection by adult
754 European sardine (*Sardina pilchardus*) in the NW Mediterranean Sea. *Prog Oceanogr.* 2021;196:102617.
- 755 85. Queiros Q, Saraux C, Dutto G, Gasset E, Marguerite A, Brosset P, et al. Is starvation a cause of
756 overmortality of the Mediterranean sardine? *Mar Environ Res.* 2021;170:105441.
- 757 86. Barroeta Z, Olivar MP, Palomera I. Energy density of zooplankton and fish larvae in the southern Catalan
758 Sea (NW Mediterranean). *J Sea Res.* 2017;124:1-9.

759
760

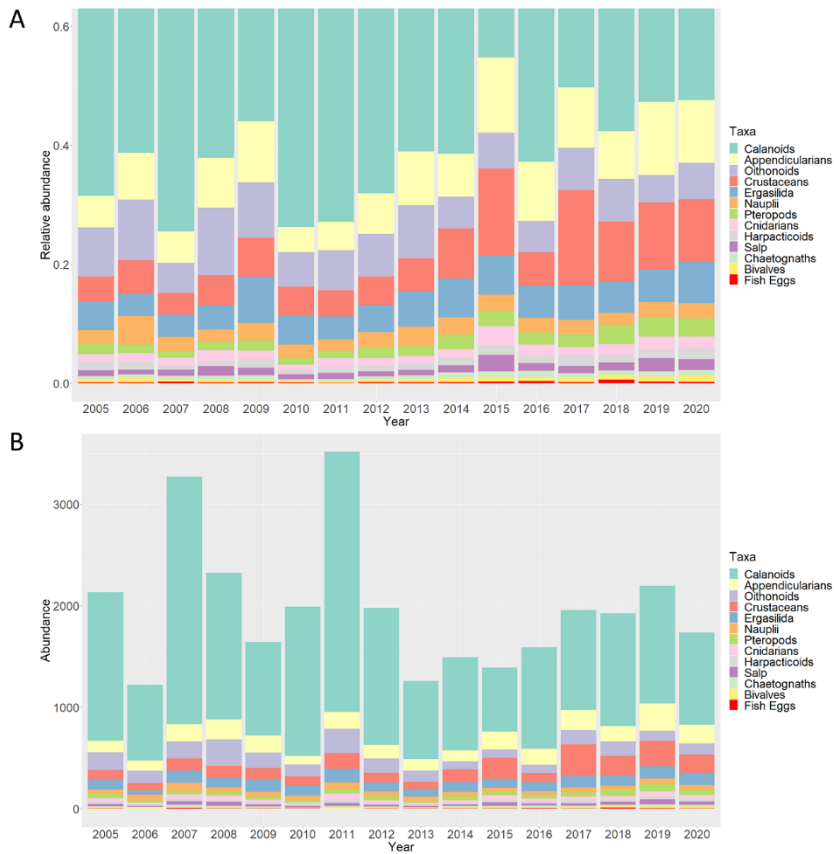


761
762 Fig. 1



763

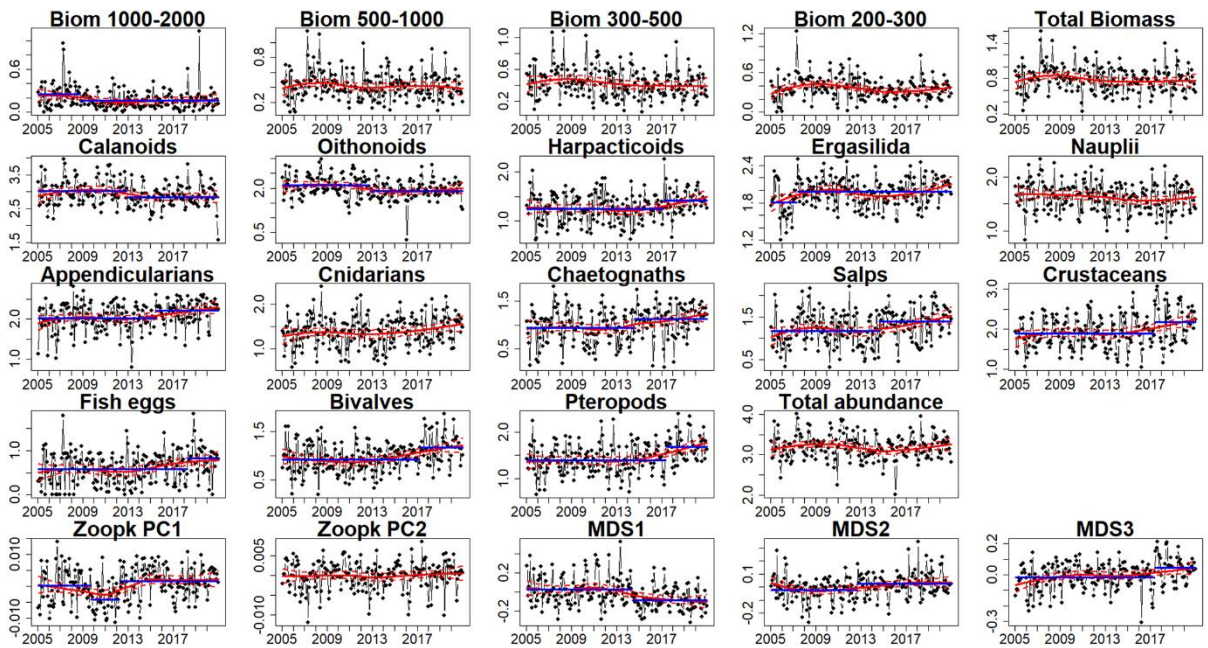
764 Fig. 2



765

766

Fig. 3

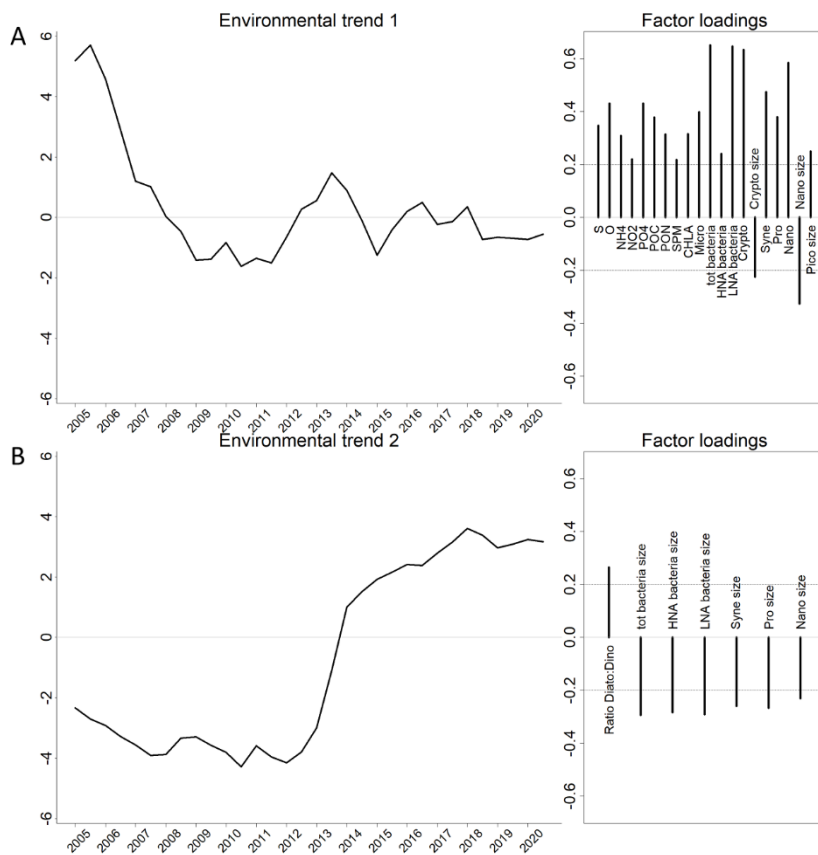


767

768

769

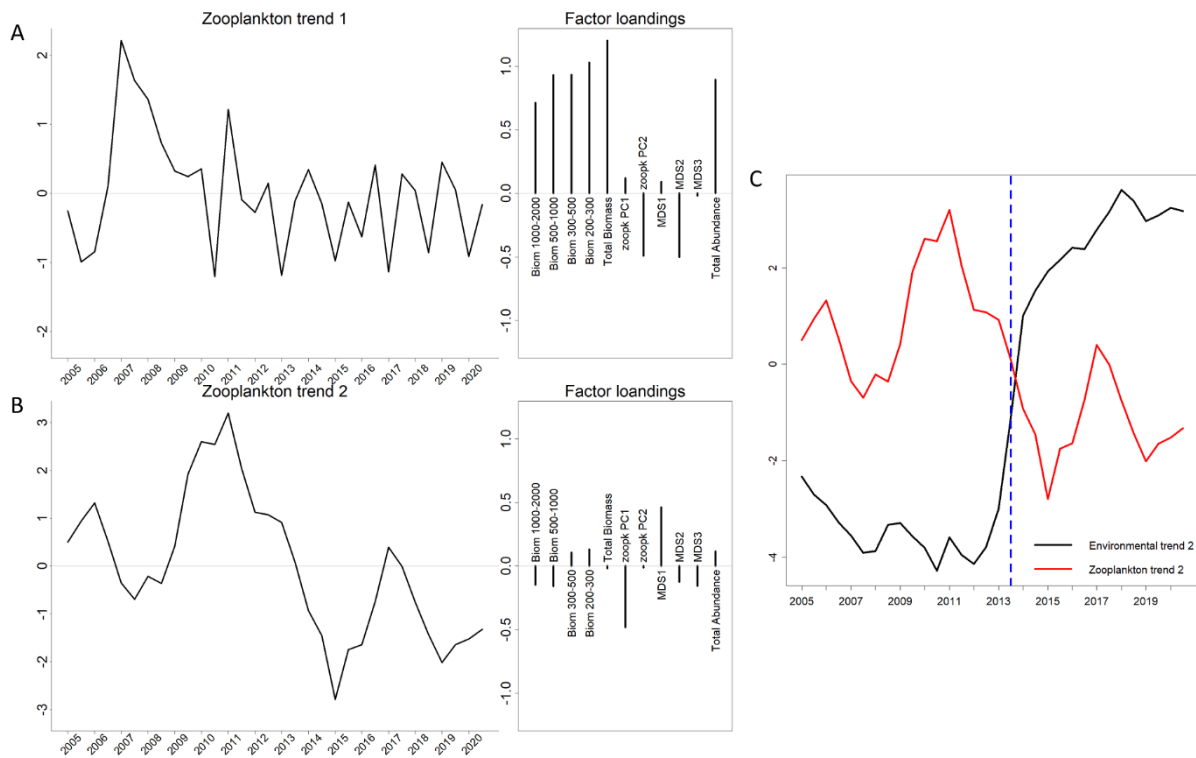
Fig. 4



770

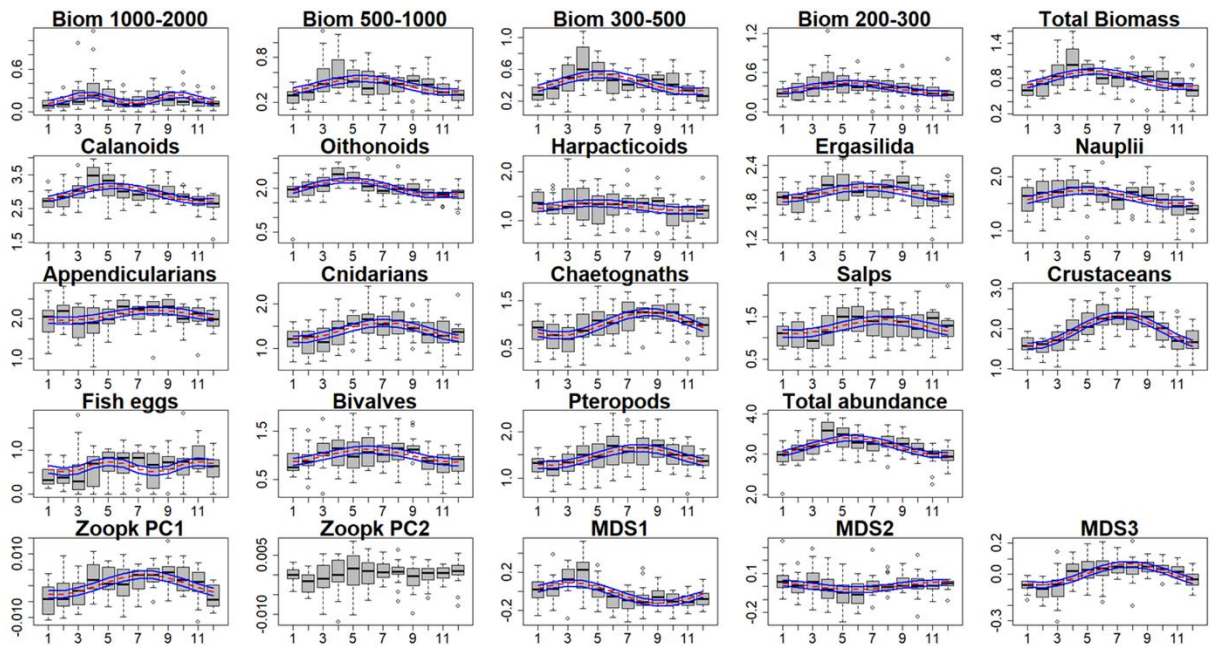
771 Fig.5

772



773

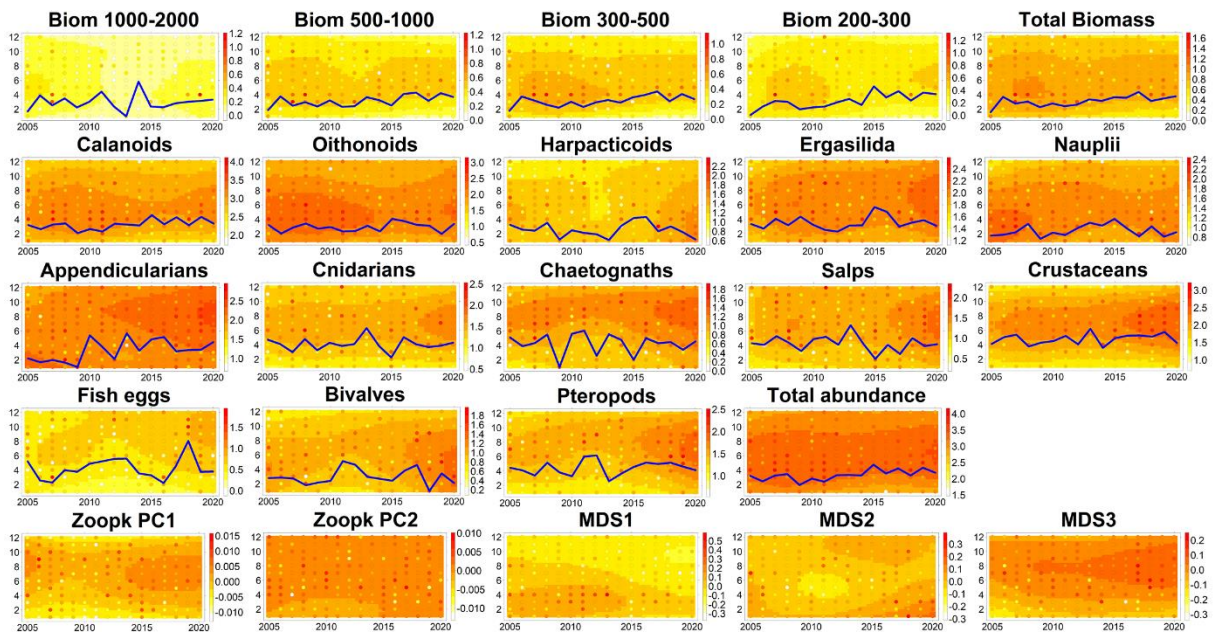
774 Fig. 6



775

776 Fig. 7

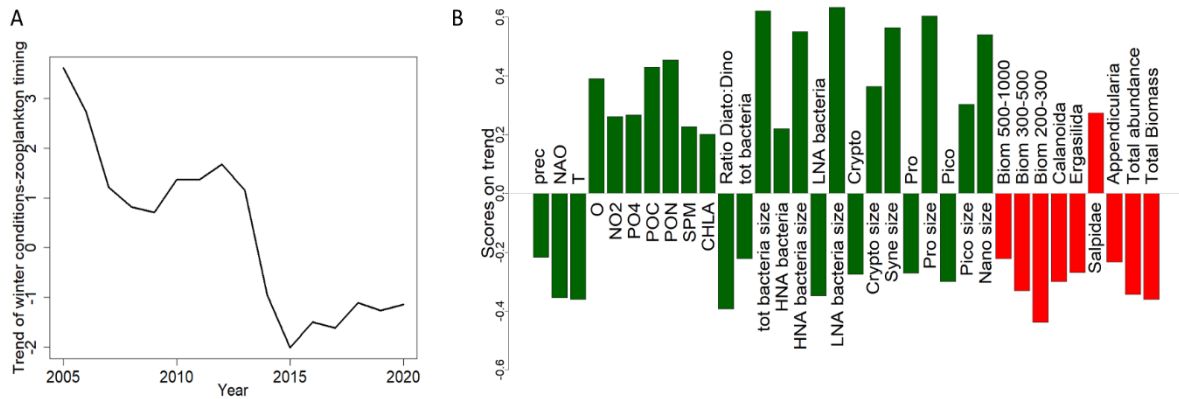
777



778

779 Fig. 8

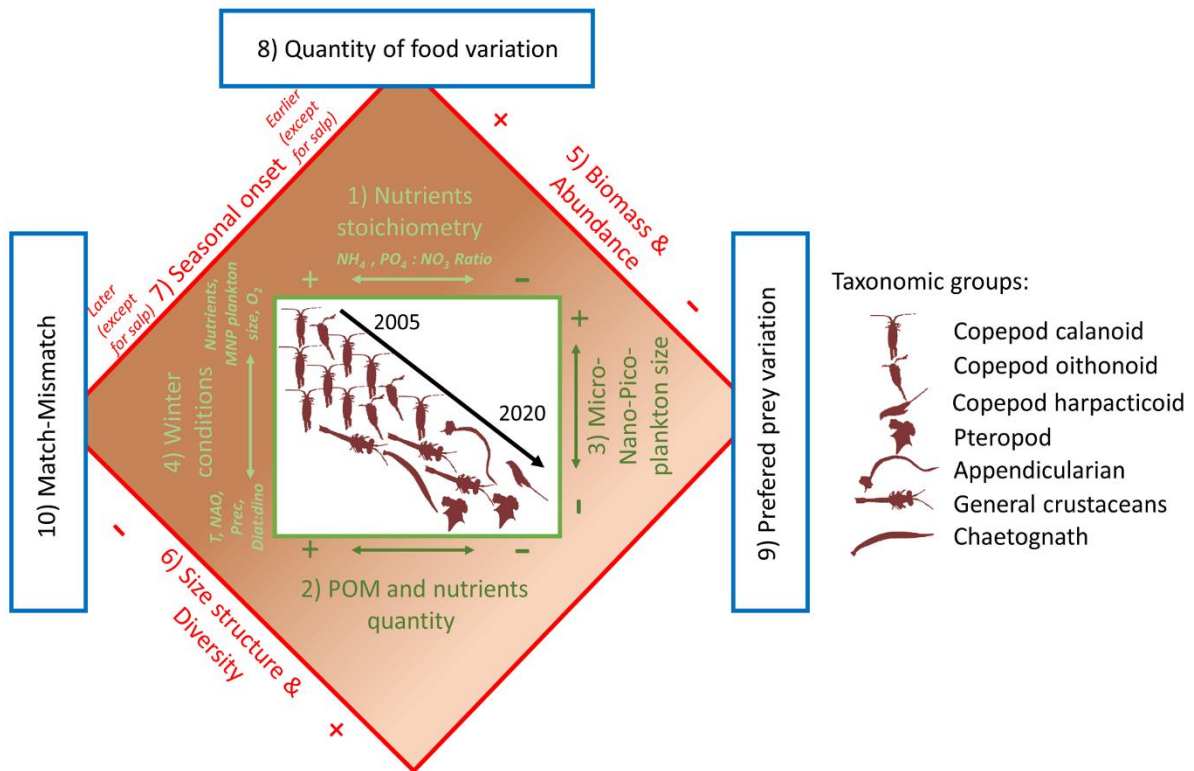
780



781

782 Fig. 9

783



784

785 Fig. 10

786